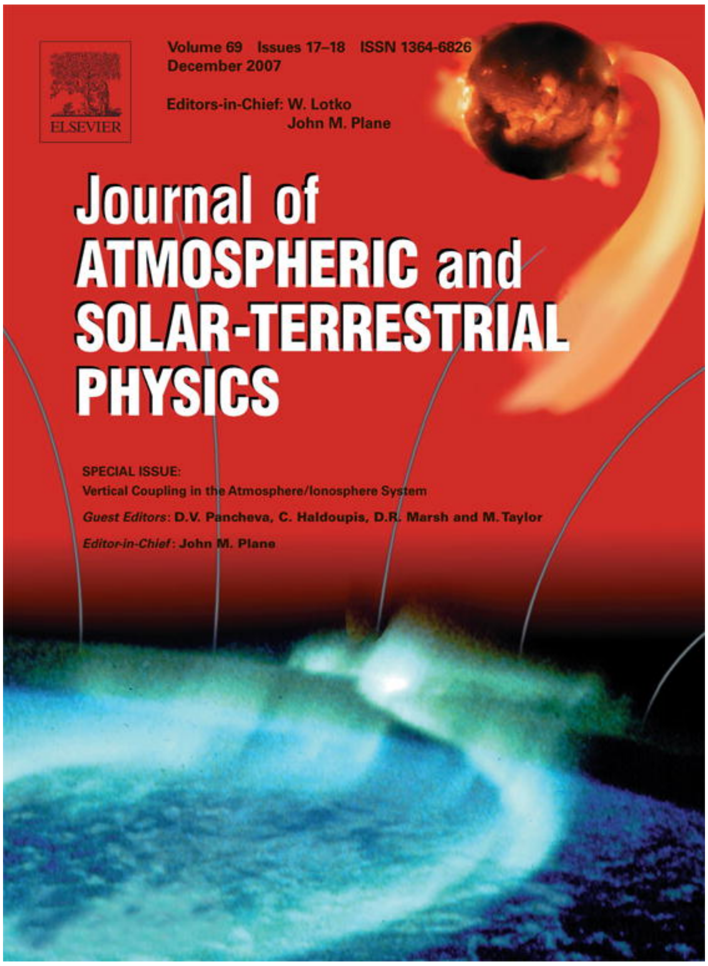
Volume 69 Issues 17–18 ISSN 1364-6826
December 2007
Editors-in-Chief: W. Lotko
John M. Plane
ELSEVIER
Journal of
ATMOSPHERIC and
SOLAR-TERRESTRIAL
PHYSICS
SPECIAL ISSUE:
Vertical Coupling in the Atmosphere/Ionosphere System
Guest Editors: D.V. Pancheva, C. Haldoupis, D.R. Marsh and M. Taylor
Editor-in-Chief: John M. Plane

ELSEVIER

Journal of Atmospheric and Solar-Terrestrial Physics 69 (2007) 2292–2308

Journal of ATMOSPHERIC AND SOLAR-TERRESTRIAL PHYSICS

www.elsevier.com/locate/jastp

Interhemispheric comparison of mesospheric ice layers from the LIMA model

F.-J. Lübken*, U. Berger

Leibniz-Institute of Atmospheric Physics, Kühlungsborn, Germany

Received 15 February 2007; received in revised form 21 May 2007; accepted 14 July 2007
Available online 25 July 2007

Abstract

The new LIMA/ice model is used to study interhemispheric temperature differences at the summer upper mesosphere and their impact on the morphology of ice particle related phenomena such as noctilucent clouds (NLC), polar mesosphere clouds (PMC), and polar mesosphere summer echoes (PMSE). LIMA/ice nicely reproduces the mean characteristics of observed ice layers, for example their variation with season, altitude, and latitude. The southern hemisphere (SH) is slightly warmer compared to the NH but the difference is less than 3 K at NLC/PMC/PMSE altitudes and poleward of 70°N/S. This is consistent with in situ temperature measurements by falling spheres performed at 69°N and 68°S. Earth's eccentricity leads to a SH mesosphere being warmer compared to the NH by ~2−3 K up to approximately 85 km and fairly independent of latitude. In general, NH/SH temperature differences in LIMA increase with decreasing latitude and reach ~10 K at 50°. The latitudinal variation of NH/SH temperature differences is presumably caused by dynamical forcing and explains why PMSE are basically absent at midlatitudes in the SH whereas they are still rather common at similar colatitudes in the NH. The occurrence frequency and brightness of NLC and PMC are larger in the NH but the differences decrease with increasing latitude. Summer conditions in the SH terminate earlier compared to NH, leading to an earlier weakening and end of the ice layer season. The NLC altitude in the SH is slightly higher by 0.6–1 km, whereas the NLC altitudes itself depend on season in both hemispheres. Compared to other models LIMA/ice shows smaller interhemispheric temperature differences but still generates the observed NH/SH differences in ice layer characteristics. This emphasizes the importance of temperature controlling the existence and morphology of ice particles. Interhemispheric differences in NLC/PMC/PMSE characteristics deduced from LIMA/ice basically agree with observations from lidars, satellites, and radars.

Keywords: Polar summer mesosphere; Ice layers; Interhemispheric differences; Numerical modeling; Noctilucent clouds

1. Introduction

Ice layers in the summer mesopause region are sensitive indicators for background conditions, in particular for temperatures and water vapor concentration (see, e.g., Siskind et al., 2005; Lübken et al., 2007). They are therefore well suited to study interhemispheric differences in an atmospheric region where direct temperature measurements are difficult and sparse. First indications of a systematic interhemispheric difference of ice layers came from VHF radar observations of (polar) mesosphere summer echoes, (P)MSE, which are closely related

*Corresponding author. Tel.: +49 38293 68100.
E-mail address: luebken@iap-kborn.de (F.-J. Lübken).

1364-6826/$ - see front matter © 2007 Elsevier Ltd. All rights reserved.
doi:10.1016/j.jastp.2007.07.006

to the presence of charged ice particles (see Rapp and Lübken, 2004, for a recent review on PMSE measurements and theory). A comparison of PMSE measurements showed that they are significantly weaker and less abundant at 62°S compared to observations at similar colatitudes in the northern hemisphere (NH) (Balsley et al., 1993; Woodman et al., 1999; Bremer et al., 2006). As was shown later, the occurrence of PMSE in the southern hemisphere (SH) increases rapidly with latitude which reduces the interhemispheric difference at ~70°N/S (Morris et al., 2004). It should be noted that apart from ice particles other geophysical parameters such as neutral air turbulence and ionization influence PMSE. Little is known about any interhemispheric difference of turbulence at mesopause altitudes. Furthermore, radars have different sensitivities which requires careful calibration before a detailed comparison can be performed (Latteck et al., 2007).

Since many years ice layers in the summer mesopause region known as 'noctilucent clouds' (NLC) are reported from ground based observers by naked eye (Leslie, 1885). Similar observations of NLC are very seldom in the SH because the geographical region where they can be observed by naked eye (50−60° latitude) is sparsely populated which prohibits a reliable NH/SH comparison. Since the early 1980s NLC can be observed by lidars which allows to study their morphology and their latitudinal distribution way into the sun-lit polar region (Hansen et al., 1989; Thayer et al., 1995; Fiedler et al., 2003). Lidar measurements of NLC in the SH are performed since the summer 1999/2000 and have recently been summarized by Chu et al. (2006). There are some indications of a systematic NH/SH difference in NLC. However, the SH data base is still sparse, and inter-annual variations and differences in the instrumental capabilities and specifications hamper a direct comparison. We will come back to a NH/SH comparison of NLC in Section 4.

Ice layers in the summer mesosphere are also observed from satellites and are called 'polar mesospheric clouds' (PMC) (Donahue et al., 1972). Various satellite borne instruments have been used to study interhemispheric differences of ice layer occurrence frequencies, brightness, etc. (e.g., Thomas, 1991; Carbary et al., 2001; Bailey et al., 2005; DeLand et al., 2006). The advantage of these techniques is that both hemispheres are covered by the same instrument. However, measurements are normally performed under different scattering angles (forward versus backward scattering) which requires careful modeling before NH/SH comparisons can be made. Still, there is some evidence that a NH/SH asymmetry in PMC occurrence and brightness exists, with PMC being more frequent and brighter in the NH. It should be noted, though, that various instrumental and geometrical corrections are applied and that not all data sets show an unambiguous and clear NH/SH difference (see discussion in Section 4).

Some 2-d model results on interhemispheric temperature differences are published by Siskind et al. (2003). At high latitudes and below the mesopause they find a much warmer southern hemisphere (up to 15 K) compared to the NH (see their Fig. 1). They later use this result to study the effect on ice layers (Siskind et al., 2005). Different from their model, LIMA predicts smaller NH/SH temperature differences (see below) and the ice model interactively couples with the 3-d transport of ice particles, water vapor, etc. Some results on NH/SH deviations in ice layers are comparable but we also find significant dissimilarities due to differences in temperatures and transport. Furthermore, we extend the NH/SH comparison by determining additional ice layer parameters, for example occurrence rates varying with season and latitude.

The purpose of this paper is to use the recently developed GCM model LIMA (Leibniz Institute Middle Atmosphere Model) to study interhemispheric similarities and differences in the background atmosphere (in particular temperatures) and their effect on ice particles. The model is described in more detail in Berger (2007) and first results have been published in Berger and Lübken (2006). We will compare the model results with a collection of falling sphere (FS) temperature measurements performed in both hemispheres and with ice particle related observations by lidars, radars, and satellites.

2. Interhemispheric comparison of summer mesosphere temperatures

A new 3-d GCM model called LIMA (Leibniz Institute Middle Atmosphere Model) has recently been developed (Berger, 2007). It covers the height range 0–150 km on a global scale and contains the most important relevant physical and chemical processes, such as dynamics, radiation, chemistry, and transport. The model applies a time step of 150 s and a triangle grid structure with 41 248 grid points. The horizontal and vertical resolution is approximately 110 and 1 km, respectively. In the height range 0–35 km the model is 'nudged' to the ECMWF/ERA-40 data (European Center for Medium Range Weather Forecasts, Reanalysis Version 40) every 6 h which introduces spatial and temporal variability. We use the same trace gas distribution and chemistry in both hemispheres. LIMA temperatures nicely agree with experimental climatologies, for example with the data set derived from FS measurements at 69°N (Lübken, 1999). In Fig. 1 we compare a midsummer temperature profile from this climatology with LIMA. As can be seen LIMA complies with mean temperatures from FS and exhibits variability around the mean. Most important, temperatures in the mesopause region are reproduced by LIMA which is crucial for ice particles. In Fig. 2 we show a latitudinal cross section of daily zonal mean temperatures in the NH mesopause region in summer (July 5, 2003). At polar latitudes the mesopause is located at approximately 87–89 km and is as cold as 125–135 K, consistent with observations. At the lower edge of ice layers, namely at ~82 km, temperatures are close to 150–155 K, in agreement with observations (Lübken et al., 1996). A 3-d Lagrangian ice transport model is superimposed on LIMA which allows to study the formation and life cycle of ice particles in the polar mesopause region including modules for a simplified mesospheric chemistry and transport of water vapor, and a Lagrangian transport and microphysics of ice particles (Berger and von Zahn, 2002; von Zahn and Berger, 2003). The ice transport model itself requires a nearly continuous initialization (once per hour) of atmospheric 3-d background winds, temperatures, air pressure, and densities which are provided by either our former COMMA/IAP model (Berger and von Zahn, 2002, 2007; von Zahn and Berger, 2003) (COMMA/IAP = Cologne Model of the Middle Atmosphere/Institute of Atmospheric Physics) or by LIMA (Berger and Lübken, 2006).Furthermore, water vapor data must be provided at the spatial boundaries of the ice model domain (78–94 km in altitude, 37.5−90°N/S in latitude) to specify boundary conditions of the water vapor transport scheme inside the ice model domain. We use water vapor background conditions from Sonnemann and Grygalashvyly (2005).

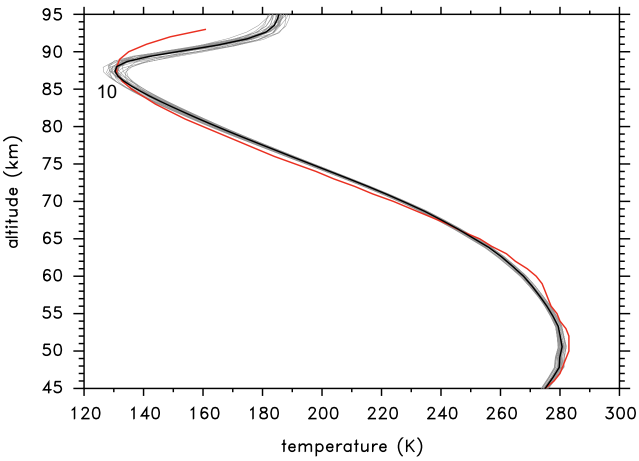

Fig. 1. Comparison of LIMA hourly temperatures from July 5, 2003 at 69°N, 16°E with a climatology published by Lübken (1999) (red line). The gray lines show individual profiles for every hour, and the black line is the mean of the gray profiles.

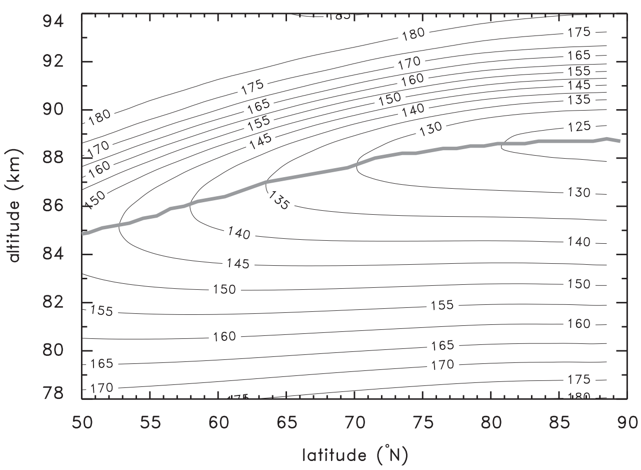

Fig. 2. LIMA temperatures (daily zonal mean) as a function of latitude and altitude for midsummer (July 5, 2003). The thick gray line indicates the altitude of the mesopause.

The combination of the Lagrangian ice transport model with LIMA background conditions is called LIMA/ice. In order to calculate ice cloud formation during a full length of a summer season LIMA/ice starts at May 15th for a northern summer season, and November 15th for a southern summer season. LIMA/ice initializes the mesopause region with an ensemble of 20 million condensation nuclei (CN). We assume that at the time of model initialization these CN exist in number densities and size distribution similar to the results from Hunten et al. (1980). This distribution is characterized by comprising only particles with radii between 1.5 and 3.5 nm with a large majority of all particles with radii of 1.5–2.0 nm. After initialization we investigate the time-dependent transport of CN in 3-d during a full summer season until August 25th (NH) and February 25th (SH), respectively. LIMA/ice follows the trajectories of each of the 20 million particles with high temporal resolution (every 45 s) while they are transported by LIMA background winds, particle eddy diffusion, and sedimentation. As in our latest 3-d version of ice modeling with COMMA/IAP (von Zahn and Berger, 2003) we have used eddy coefficients after Lübken (1997) but reduced by a factor of 2.

During transport, formation of ice on CN may occur by heterogeneous nucleation. The water vapor saturation pressure over ice is computed using LIMA temperatures and the laboratory data according to Mauersberger and Krankowsky (2003). We note that a different expression is favored by Rapp and Thomas (2006) following measurements by Murphy and Koop (2005). Unfortunately, no measurements of water vapor pressure over ice at mesospheric conditions are yet available. We have decided to use the expression from Mauersberger and Krankowsky (2003) since it gives better results in LIMA/ice regarding the seasonal coverage and the latitudinal extent (using the Murphy and Koop expression gives too short seasons and limits the ice layers too much to polar regions).

The formation as well as sublimation of ice is interactively coupled to the background water vapor which thereby leads to a redistribution of H_2O known as 'freeze drying'. Finally, we take into account the temperature deviation between a large ice particle and the atmospheric background (see section 'particle temperature' in Rapp and Thomas, 2006). During the ice model run, a number of dynamical processes cause a continuous loss of CN from the ice model domain. This loss of CN is compensated for by a local production of CN ('relocation') described in detail in von Zahn and Berger (2003).

Due to computer resource limitations we have run LIMA/ice for two selected years only. We have chosen the summers of 2001 (NH) and 2004/05 (SH) for reasons explained later. Results from these two years will mainly be used for interhemispheric comparison in this paper. We have also run a less sophisticated version of LIMA/ice using classes of ice radii only (and not individual particles). These model runs showed similar NH/SH results for other years which indicates that our conclusions for 2001 and 2004/05 are of general relevance (Berger and Lübken, 2006).

The appropriateness of LIMA/ice to study ice particle morphology is best demonstrated by comparison with observations. In Fig. 3 we show the altitude distribution of the NLC peak heights at 69° in the NH and SH, respectively. More precisely, the distribution of centroid altitudes z_c of backscatter coefficients (BSCs) larger than $1 \times 10^{-10}/(\mathrm{sr\,m})$ averaged over the summer seasons is

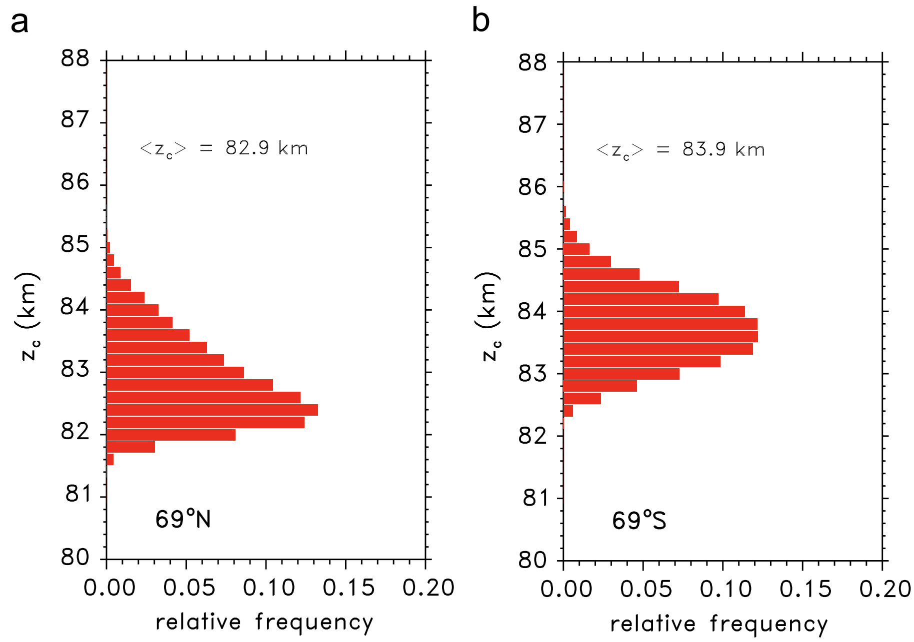

Fig. 3. Left: The altitude distribution of NLC at 69° in the NH (left) and SH (right) determined from LIMA/ice. More precisely the occurrence frequency of centroid altitudes of BSC larger than $1 \times 10^{-10}/(\mathrm{sr\,m})$ averaged over the summer seasons of 2001 (NH) and 2004/05 (SH) is shown. The median altitudes are 82.9 km (NH) and 83.9 km (SH).

shown. The BSCs indicate the strength of the lidar signal and are calculated for a typical lidar wavelength of $\lambda = 532\,\text{nm}$ (see Fiedler et al., 2003, for a definition of BSC). We have used a lower limit of $\text{BSC} = 1 \times 10^{-10}/(\text{sr m})$ to reflect typical sensitivities of modern lidar systems. The median height of the z_c distribution from LIMA/ice is 82.9 km in the NH which is in nice agreement with the median height of 83.2 km observed by our Rayleigh/MIE/Raman lidar located at the Arctic Lidar Observatory for Middle Atmosphere Research (ALOMAR) (Fiedler et al., 2003). NLC layers are found between approximately 82 and 85 km in both hemispheres, consistent with observations. The observed height distribution is rather symmetric around the mean in the SH, whereas the distribution is somewhat skewed in the NH. This skewness in the NH is to a large extent caused by a seasonal variation of NLC heights which is larger in the NH compared to the SH (see discussion in Section 4).

As a second comparison we show in Fig. 4 the seasonal variations of PMSE occurrence frequencies from the ALOMAR wind radar (ALWIN, 69°N, 16°E) and from the Davis VHF radar (69°S, 78°E). In the same figure we show daily local PMSE occurrence rates from LIMA/ice at the same locations. More details about ALWIN and the Davis VHF radar are published in the literature (Bremer et al., 2006; Morris et al., 2004). PMSE in LIMA/ice is determined from a proxy defined as $P \sim r_A^2 \cdot Z_A \cdot N_A$, where r_A is the particle radius, Z_A their charge, and N_A their number density (Rapp et al., 2003). The daily local occurrence rate is determined as follows: at a certain location and within a latitudinal/longitudinal box of $1^\circ/3^\circ$ we determine the number of hours per day where the proxy anywhere within a vertical column is larger than a certain threshold. We have chosen a somewhat arbitrary threshold of $P = 10^5\,\text{nm}^2 \times Q_e/\text{ccm}$ to reflect the overall morphology of PMSE (the ice particle charge is 1 Q_e in all cases; Q_e is the elementary charge). It is important to note, however, that the same threshold is used for all studies in this paper, i.e., for all seasons, all latitudes and longitudes, both hemispheres, etc. It is known that neutral air turbulence is a key element in producing PMSE but this is not covered by the proxy. As can be seen from Fig. 4 LIMA/ice reproduces the general features of the seasonal variation of PMSE occurrence at 69°N and also the maximum values in midsummer of approximately 80–90%. In Fig. 4 we also show the PMSE occurrence frequencies at the Antarctic station Davis (Morris et al., 2004; Latteck et al., 2007) and LIMA/ice simulations for the same location. The season in the SH ends earlier in LIMA/ice whereas the beginning is at approximately the same time both in LIMA/ice and in observations. We note that the beginning of the PMSE season is somewhat late in LIMA/ice (in both hemispheres) compared to observations. From our preliminary LIMA/ice runs for other years we find that the start of the season varies from year to year. We do not know yet whether the discrepancy between LIMA/ice and observations regarding the

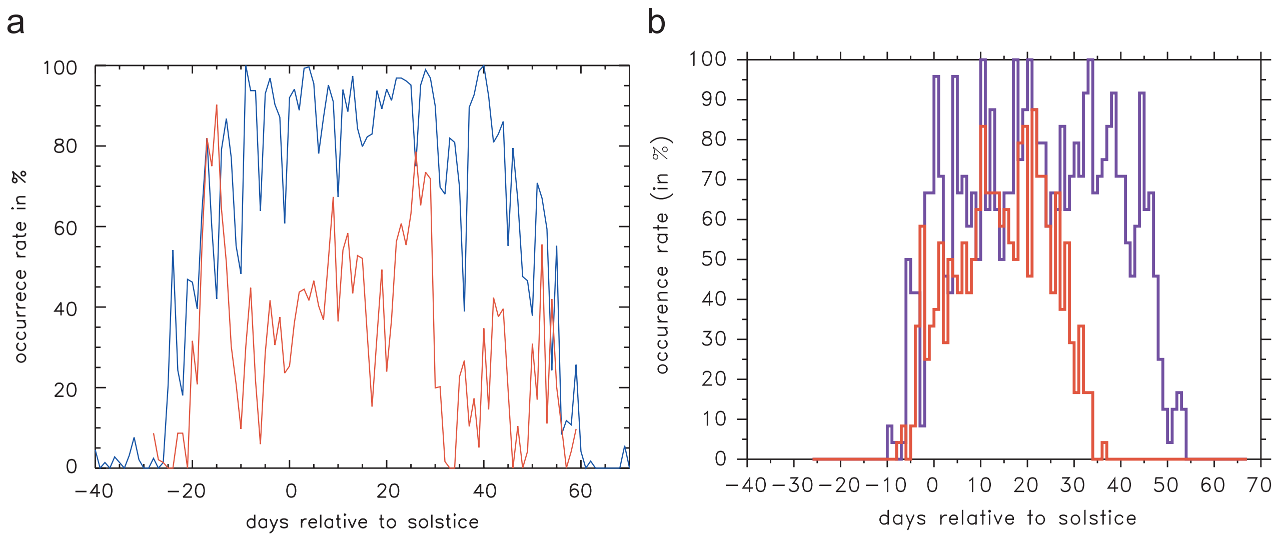

Fig. 4. Left: ALWIN VHF radar measurements of PMSE at 69°N, 16°E (blue) and VHF radar measurements at Davis at 68°S, 78°E (red) for the summer seasons of 2001 and 2004/05, respectively (after Latteck et al., 2007). Right: daily local PMSE occurrence frequencies from LIMA/ice at the same locations in the same years. See text for more details on the definition of daily local PMSE occurrence rates.

beginning of the PMSE season is persistent. A systematic study of the lengths of the PMSE (and NLC) seasons requires that LIMA/ice model results from several years covering the entire season are available, which is not yet the case. We note that several factors might vary with season which influence PMSE but are not yet embedded in LIMA/ice, for example turbulence, water vapor concentrations at the latitudinal and height boundary of the ice domain, geomagnetic effects, etc. We will discuss the NH/SH difference of PMSE in more detail in Section 4.

The nice agreement of various ice layer parameters in LIMA/ice with observations from different techniques demonstrates that LIMA correctly describes the main features of the background atmosphere. It also suggests that the microphysical processes involved in ice particle generation, transport, and sublimation, are correctly represented in LIMA/ice.

We now study interhemispheric differences in the background atmosphere and concentrate on temperatures in the summer region. In Fig. 5 we show temperature profiles at 69°N/S for the years 2001–2005. The summers in the southern hemisphere are designated by the year in the latter part of summer. For example, the SH summer from December 2000 to February 2001 is labeled '2001'. Generally speaking the mesopause region is somewhat warmer and lower in the SH, but the difference is a few Kelvin and less than 1 km only (the mean mesopause altitude and temperature differ by

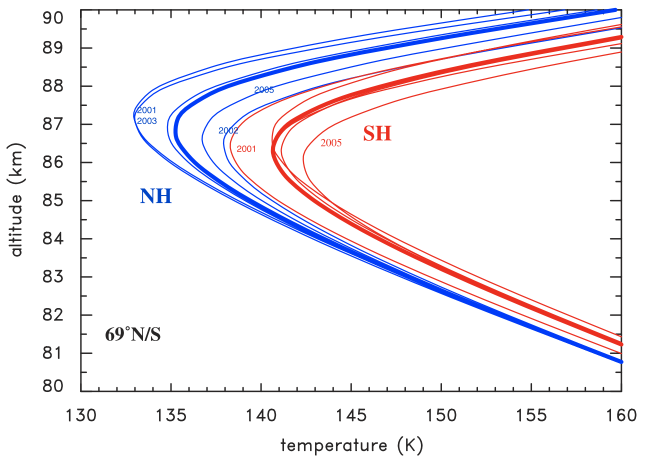

Fig. 5. LIMA model results of temperature profiles at 69°N latitude in the northern (blue) and southern (red) hemisphere for various years indicated in the plot. The SH summers are labeled according to the later part of the summer (e.g. '2005' for the summer of 2004/2005). Monthly mean profiles for July (NH) and January (SH) are shown.

~600 m and ~5 K, respectively). At typical NLC/PMSE altitudes (83–85 km) the difference of mean temperatures is very small (~2−3 K). The interannual variability of temperatures at the mesopause is several Kelvin in both hemispheres, decreasing with decreasing altitude. This implies that a NH/SH comparison of ice layer observations from single years may not reflect the mean difference in the thermal structure. At mesopause altitudes the warmest year in the NH is as warm as the coldest year in the SH. For the NH/SH ice layer comparison presented below we have chosen the years 2001 (NH) and 2004/05 (SH) since these years highlight the general difference in the thermal structure.

In Fig. 6 (upper panel) we show hemispheric differences of five year mean temperatures in the polar mesopause region in midsummer (SH minus NH, i. e., January minus July) as a function of latitude. In the altitude range of ice layers (80–90 km) the SH is warmer by 1−10 K. The difference is largest around the mesopause and increases with decreasing latitude. At midlatitudes, for example at Kühlungsborn (54°N) where MSE and NLC are observed with an average occurrence frequency of 5–10% and ~5%, respectively (Zecha et al., 2003; Gerding et al., 2007), the mesopause region in the NH is colder by up to 10 K compared to corresponding SH colatitudes. The larger temperatures in the SH at these latitudes drastically reduce the ice particle occurrence rate and basically eliminates the chance to observe ice layers. We will discuss potential reasons for the NH/SH temperature difference in Section 4.

In Fig. 6 (lower panel) we show NH/SH temperature differences from LIMA in the latitude band 65−70° in the altitude range 30–95 km for direct comparison with HALOE results (see Figure 7 in Hervig and Siskind, 2006). Below ~70 km both LIMA and HALOE show a SH being warmer by ~3−5 K. Around 75 km HALOE observes a maximum of approximately 7 K which is not present in LIMA. We speculate that this could be caused by a NH/SH difference in trace gas distributions. In the altitude range of ice layers (80–90 km) LIMA shows the SH to be warmer by up to 10 K at 88 km, partly caused by a shift of the mesopause height (see Section 4.1). This height range is above the range covered by HALOE.

3. Interhemispheric difference of ice layers

We now study the effect of the NH/SH temperature difference on ice layers. In Fig. 7 we show

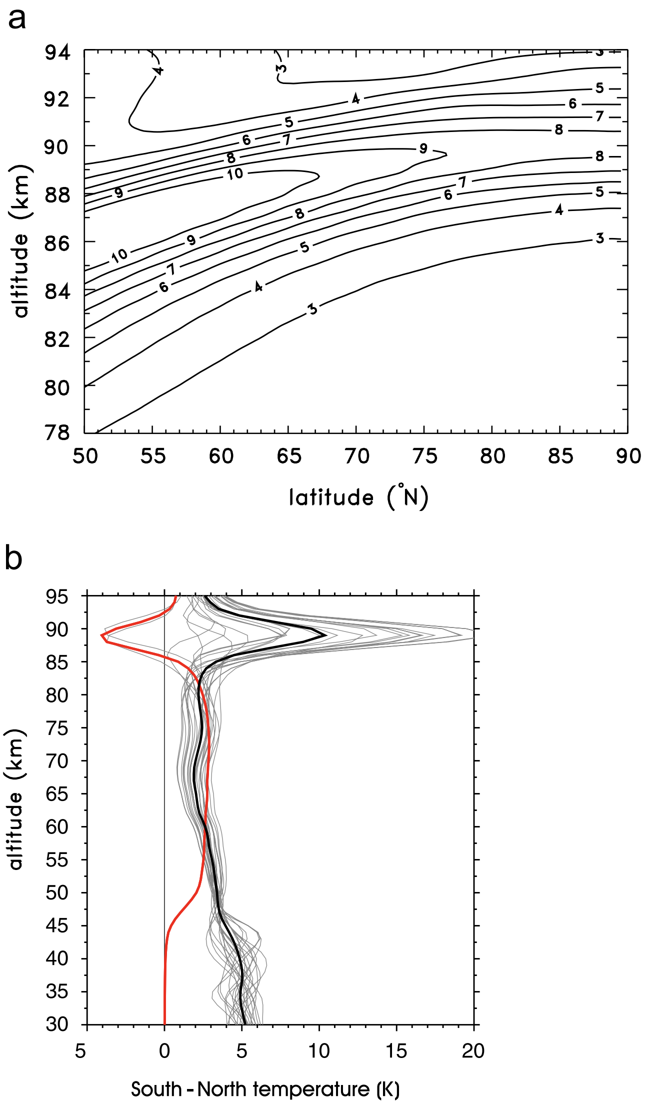

Fig. 6. Upper panel: Hemispheric temperature difference in the polar summer mesopause region from LIMA (SH minus NH, mean January minus mean July) averaged over 5 yr. Temperatures are generally larger in the SH. Lower panel: SH minus NH temperature differences from LIMA within a latitude band of 65°–70° for comparison with HALOE. The thin lines are monthly mean averages (January minus July) of single summer seasons (2001 minus 2005). The thick line presents the mean of all individual profiles. The red line shows the SH–NH temperature difference caused by the eccentricity of Earth's orbit for 2006 (see also Fig. 13).

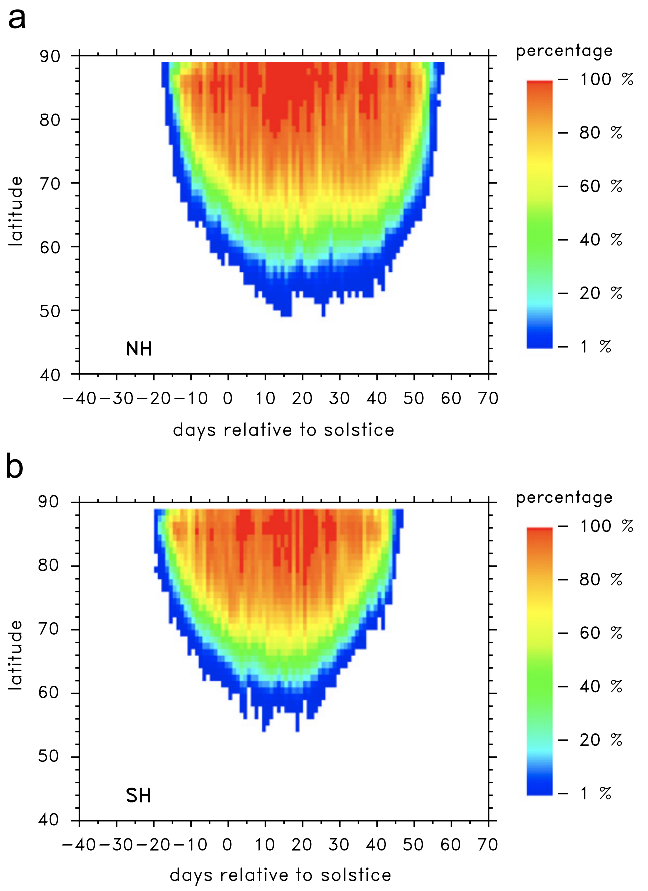

Fig. 7. Occurrence rates (daily zonal mean) of PMSE as a function of latitude and season in the NH summer of 2001 (upper panel) and in the SH summer of 2004/05 (lower panel). See text for more details on the definition of the PMSE proxy and occurrence rates.

LIMA/ice simulations of daily zonal mean PMSE occurrence rates in the NH and SH, respectively. This occurrence rate is determined as follows: within a given latitude band of 1° width and at a given hour we count the number of longitudinal segments of width 3° where the proxy anywhere within a vertical column is larger than a threshold and divide by the total number of segments (= 120). This procedure is repeated for all 24 h of a day. The relative occurrence is taken as the average over all 24 h. The final result is the zonally averaged occurrence rate of PMSE. As expected, the occurrence frequency increases towards polar latitudes in both hemispheres. PMSE are practically permanently present in both hemispheres from the pole to ~75° and basically disappear equator-ward of approximately 50°N and 60°S, respectively. They extend further equator-ward in the NH compared to SH.

In Fig. 8 we show LIMA/ice results of the seasonal variation of PMSE occurrence frequencies at 54°, 69°, and 78° in the northern and southern hemispheres. We have chosen these latitudes for easy comparison with our radar and lidar measurements at Kühlungsborn (54°N), ALOMAR (69°N), and Spitsbergen (78°N). LIMA/ice predicts an increase of PMSE from mid to polar latitudes. Indeed, measurements show typical occurrence rates of 5–10%, 80–90%, and ~100% at these stations

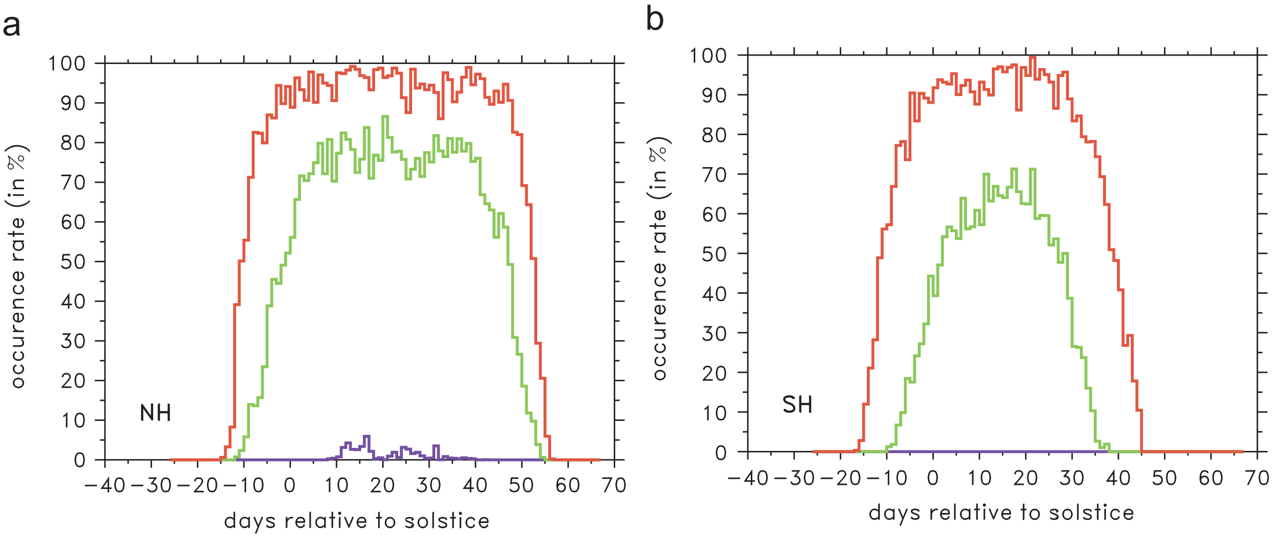

Fig. 8. Occurrence frequency (daily zonal mean) of PMSE from LIMA at 54° (blue), 69° (green) and 78° (red) as a function of season in the NH summer of 2001 (left) and in the SH summer of 2004/2005 (right).

(Zecha et al., 2003; Bremer et al., 2006; Lübken et al., 2004b) in nice agreement with LIMA/ice. The seasonal variation of PMSE at SH colatitudes is similar but certain differences are evident. For example, the occurrence rates are generally smaller and PMSE are totally absent at 54°S . In general, the season is shorter compared to the NH.

In Fig. 9 we show LIMA/ice results of the seasonal and latitudinal variation of NLC occurrence frequencies for the summers of 2001 (NH) and 2004/2005 (SH). The NLC occurrence rate is defined similar to PMSE (see above) and a threshold of $\mathrm{BSC} = 4 \times 10^{-10}/(\mathrm{sr\,m})$ was applied. The occurrence rate of NLC in LIMA/ice increases with increasing latitude in both hemispheres, in agreement with lidar measurements (Fiedler et al., 2003; Höffner et al., 2003; Chu et al., 2006; Gerding et al., 2007). As is well known since the early satellite observations, the occurrence frequency of PMC also increases toward the poles (see, e.g. Thomas, 1984). The NLC occurrence frequency variation with season and latitude is similar in both hemispheres, and also similar to PMSE (see Fig. 7). For example, the seasonal variation is non-symmetric around midsummer in both hemispheres (shifted towards autumn by approximately 10–15 days). NLC disappear toward low latitudes where the cutoff is more equator-ward in the NH compared to SH (similar to PMSE). Since NLC are determined by 'large' ice particles (radius approximately greater than 20 nm) whereas PMSE are less sensitive to

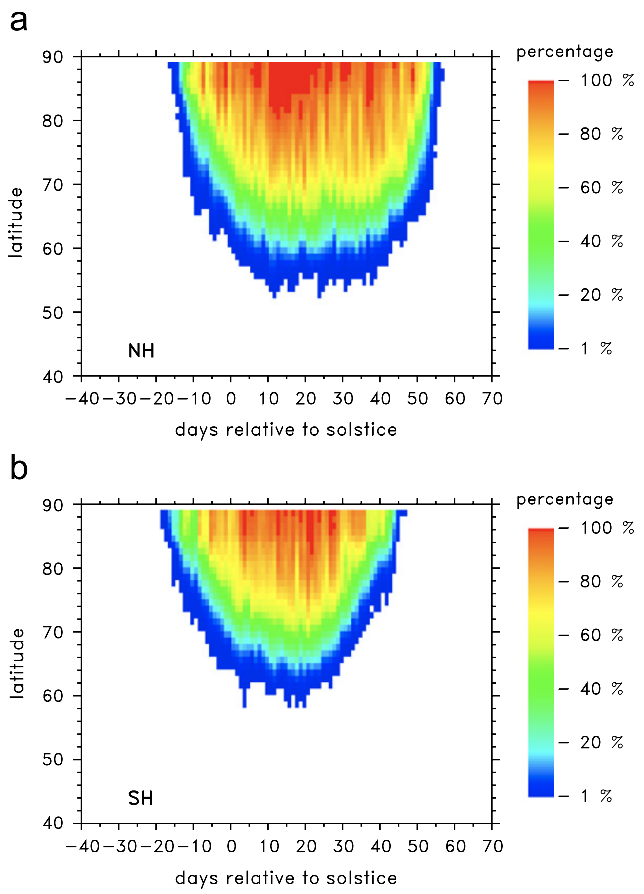

Fig. 9. Occurrence rates (daily zonal mean) of NLC with $\mathrm{BSC} > 4 \times 10^{-10}/(\mathrm{sr\,m})$ as a function of latitude and season in the NH summer of 2001 (upper panel) and in the SH summer of 2004/2005 (lower panel). See text for more details on the definition of BSC and occurrence rates.

particle size, some differences appear. This concerns the latitudinal coverage, the seasonal variation, the magnitude of occurrence rates, and the altitude distribution. Generally speaking, the NLC distribution is embedded in the PMSE distribution.

In Fig. 10 we show LIMA/ice results of the seasonal variation of NLC occurrence frequencies at 69° in the NH and SH, respectively. The variation with season is similar to PMSE. For example, both NLC and PMSE start around day −10 (relative to solstice; compare Fig. 10 with Fig. 6). At higher latitudes PMSE starts earlier compared to NLC in both hemispheres (see Figs. 7 and 9). Observations at 69°N show that PMSE start around day −30, whereas NLC start around day −20 (Bremer et al., 2006; Fiedler et al., 2005). This is significantly earlier compared to LIMA/ice which indicates that the seasonal variation of upper mesosphere temperatures and/or water vapor is presumably not represented exactly in LIMA. We note, however, that the observed beginnings of the PMSE/NLC seasons vary substantially from year to year. We will investigate in the future whether the mentioned discrepancy is due to natural variability or an indication of some systematic deficiency in LIMA/ice, for example NH/SH differences in trace gases. We note that LIMA/ice shows that NLC are less frequent than PMSE in both hemispheres, in agreement with observations.

In Fig. 11 we show LIMA/ice results of the seasonal variation of mean NLC brightness as a function of latitude in the NH and SH, respectively. We define brightness as the integral of all BSC values in an altitude column. NLC are brighter towards polar latitudes in both hemispheres. The brightness of NLC is generally larger in the NH and can differ from the SH by more than a factor of 3 at certain locations. Comparison with Fig. 9 shows that in general occurrence rates and brightness vary similarly. As might be expected the occurrence rate of NLC increases if brighter NLC are detectable. Careful inspection of both figures shows, however, that this is not always the case. For example, the brightness increases abruptly at day 10 in the NH but the occurrence frequency does not exhibit a similar sudden increase.

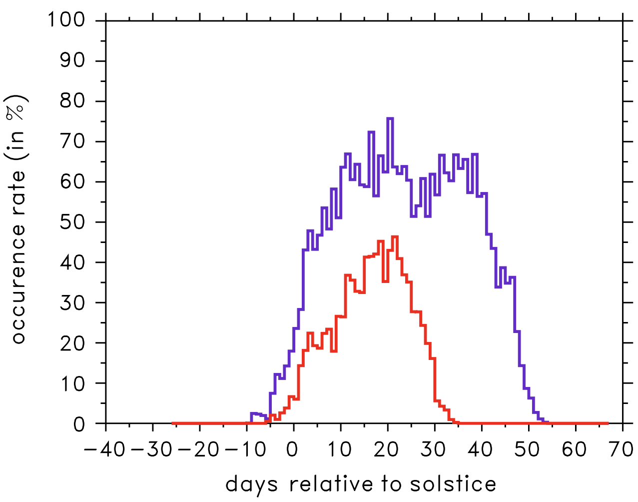

Fig. 10. Occurrence rates (daily zonal mean) of NLC with BSC > 4×10^{-10}/(sr m) at 69° latitude in the NH (blue) and SH (red) for the summer seasons of 2001 and 2004/2005, respectively.

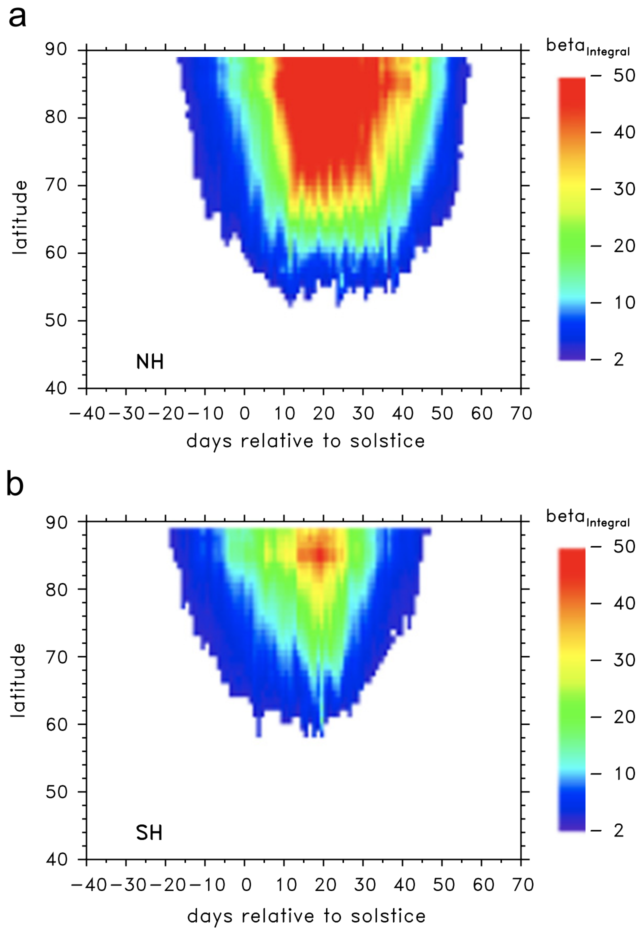

Fig. 11. Integrated NLC brightness (daily zonal mean) at 69° in the NH summer of 2001 (upper panel) and SH summer of 2004/2005 (lower panel). See text for more details on the definition of integrated NLC brightness.

In Fig. 12 LIMA/ice results of the seasonal variation of mean NLC heights as a function of latitude in the NH and SH are shown. Mean NLC heights vary with season in both hemispheres and are lower by 1–2 km in the center of the season (approximately around day 20) compared to the beginning and the end of the season. This implies

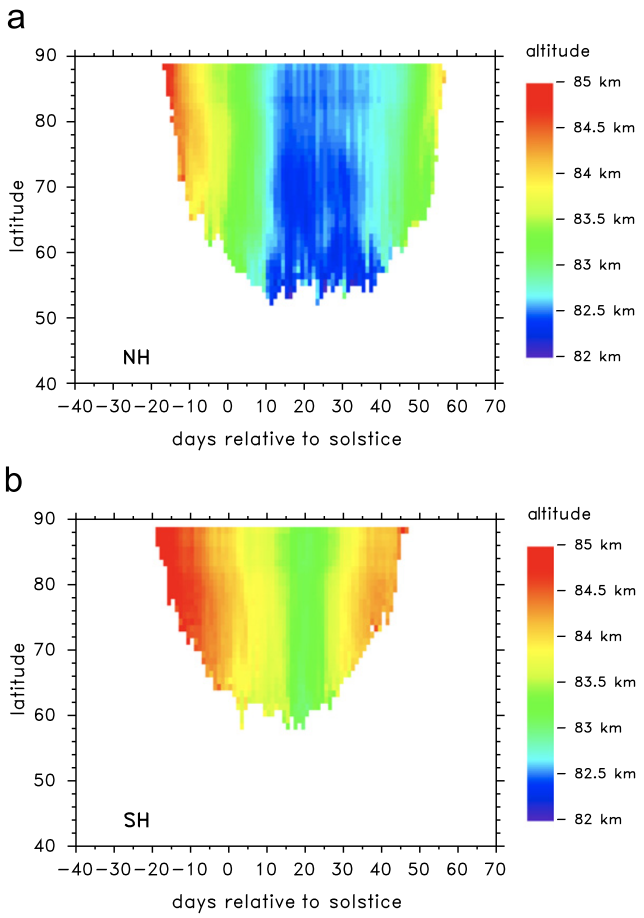

Fig. 12. Mean altitude (daily zonal mean) of NLC with BSC$>4\times10^{-10}$/(sr m) as a function of latitude and season in the NH summer of 2001 (upper panel) and in the SH summer of 2004/2005 (lower panel).

that a significant bias in mean NLC heights may occur if only a part of the season is covered by lidar and/or satellite measurements. The large NLC data set from 1997–2006 available from ALOMAR indeed shows a systematic variation of the mean NLC altitudes with season with altitudes being larger by ~1 km at the beginning and end of the season compared to the middle period (J. Fiedler, private communication; see also Section 4.2.1 for satellite observations of PMC heights). We see from Fig. 12 that NLC systematically appear at higher altitudes in the SH compared to NH, but the difference is small (typically less than 1 km; see also Fig. 3). It is interesting to note that the temperatures at the mean NLC altitudes (see Fig. 3) differ by 1–2 K. Care must be taken when comparing temperatures at particular locations since ice particle formation may take several hours during which the ice particles are transported by several hundred kilometers. They have thereby encountered different atmospheric conditions in the NH and SH. Furthermore, the nucleation of ice particles starts above NLC altitudes where temperature differences are generally larger. Therefore, the local temperature difference of 1–2 K at NLC altitudes is presumably not essential for NLC formation.

4. Discussion

4.1. Interhemispheric temperature difference: comparison with measurements and geophysical reasons

The NH/SH temperature differences shown in Figs. 5 and 6 are consistent with FS measurements performed in both hemispheres (Lübken, 1999; Lübken et al., 2004a). A NH/SH comparison of these measurements shows small differences of only 2–3 K at NLC/PMSE altitudes, increasing somewhat with height (see Figure 6 in Lübken et al., 2004a). The differences are significantly larger in the second half of July/February (SH is warmer) indicating that the summer season is shorter in the SH compared to the NH. This is also seen in LIMA and leaves its fingerprints in the ice layer morphology, for example in the length of the PMSE and NLC seasons. Both are shorter in the SH compared to NH (see Figs. 4 and 10). We note that the precision of satellite temperatures in the polar summer mesopause region is not good enough to study interhemispheric differences of a few Kelvin (see, for example, Kutepov et al., 2006, for a discussion of SABER temperatures). We have also compared zonal winds from LIMA and found no significant NH/SH difference in the mesosphere up to 70 km and poleward of 55°. This is consistent with wind measurements from FS at Andøya (69°N) and Rothera (68°S) which also show no significant difference (the FS technique works for winds only up to altitudes of ~70 km) (Müllemann and Lübken, 2005).

The main geophysical processes leading to the warmer SH are presumably differences in dynamical forcing by gravity waves (sources and/or filtering) and Rossby waves, in solar radiation due to eccentricity of the Earth's orbit, and in chemical heating caused by trace gas concentrations. We repeat that we have used the same trace gas concentrations in both hemispheres, except for water vapor which is interactively coupled to ice particles.

The LIMA model intrinsically includes wave forcing due to nudging to ECMWF in the lower atmosphere and wave filtering and breaking in the upper atmosphere. We hesitate to investigate NH/SH differences in dynamical parameters (e.g. temperature or wind variabilities) in this paper since it is not clear which part of the atmosphere must be considered. It is clear that interhemispheric differences in local variabilities may be misleading since dynamical processes can act over very large distances. For example, in the northern summer of 2002 large Rossby wave activity in the SH has significantly altered the thermal structure in the NH summer mesosphere and thereby also the occurrence of PMSE and PMC (Goldberg et al., 2004; Becker et al., 2004; Karlsson et al., 2007). In fact, with LIMA/ice we also see larger temperatures in the NH summer mesosphere in 2002 (see Fig. 5) and hence less PMSE and NLC compared to other years (not shown here). It is self-evident that a similar coupling from the NH winter to the SH summer hemisphere exists (see, e.g., Becker and Schmitz, 2003, for model studies of this effect). It is therefore unclear at the moment which part of the atmosphere can be used to characterize the dynamic variability responsible for interhemispheric differences in the thermal structure of the summer mesopause region. We will study this question in more detail in the future.

The eccentricity of the Earth's orbit leads to a 6% larger total solar irradiance in the SH summer compared to the NH summer. To investigate this effect on the mean temperatures we have reversed the Earth/Sun distance in the model, i.e., we have used the larger NH distance in the SH, and vice versa. The dynamic situation is not changed, i.e. it is taken from ERA-40 data in the NH and SH, respectively. As already mentioned in Section 2 we have used the same trace gas distribution and chemistry in both hemispheres. In Fig. 13 we show the monthly mean temperature profile from LIMA for July 2006 and also the profile when the Sun's distance to the Earth corresponds to the SH summer situation in January (solar radiation is increased by ~6%; 'mirrored case'). Indeed, the mesosphere is warmer by approximately 2 K and the mesopause is shifted upward by ~500 m. At 69° latitude and below ~85 km (and above 55 km) the NH/SH temperature differences shown in Fig. 5 and in the lower panel of Fig. 6 are nearly entirely due to the eccentricity of Earth's orbit. The atmosphere immediately above the mesopause is slightly warmer

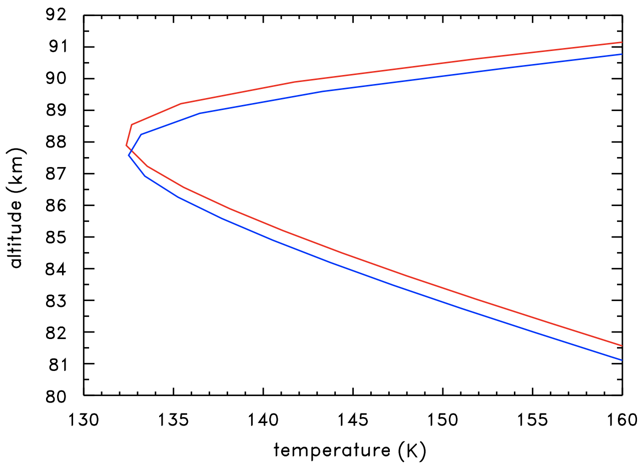

Fig. 13. Mean July temperature profiles at 69° latitude in the northern hemisphere: blue: actual conditions from 2006; red: if the Sun would be closer to the Earth leading to 6% larger total solar irradiance (as is the case in the southern hemisphere summer).

in the mirrored case due to the shift of the mesopause altitude. The eccentricity effect does not vary much for latitudes poleward of ~50°. This implies that the latitudinal variation of temperature differences shown in Fig. 6 (upper panel) are mainly due to dynamical forcing. We note that our results are very similar to the 2-d model studies by Siskind et al. (2003) (see their Fig. 12). This concerns the absolute magnitude of the effect and the variation with latitude. We have also studied the reverse case, namely comparing actual SH summer temperatures with those from an increased Sun/Earth distance. The results are similar to the NH summer but with reversed sign.

4.2. *Comparison of NH/SH ice layer differences from LIMA/ice with observations from satellites, lidar, and radar*

The main reason for the latitudinal variation of ice layer characteristics in the SH and NH is the difference in the thermal structure caused by Earth's eccentricity and by differences in dynamical forcings. Even small temperature differences of only a few degrees (for example at 69°) can cause large differences in ice layer characteristics. This emphasizes the sensitivity of ice particles to the thermal structure.

Some factors are known to influence the occurrence frequency of mesospheric clouds but are not included in LIMA/ice, for example solar proton events and rocket exhaust (von Savigny et al., 2007; Stevens et al., 2005). Very little is known about potential interhemispheric differences of such effects. We argue that these effects are of sporadic nature and do not change the general morphology of ice clouds.

In the following we also investigate the length of the PMSE/PMC/NLC seasons. We should thereby keep in mind that in LIMA/ice we have used fixed boundary water vapor values for the entire summer season, i.e. independent of time. It is known, however, that water vapor in the summer mesosphere varies with season and exhibits a maximum concentration in August (Seele and Hartogh, 1999). Although the effect of water vapor on saturation is minor compared to temperatures it may somewhat alter the seasonal variation of ice layer characteristics (e.g., brightness). Some minor differences between LIMA/ice model and observations mentioned below may be due to this effect. We plan to introduce seasonally varying water vapor boundary concentrations in the future.

We will now study in detail the comparison between LIMA/ice results and various observations of ice layers.

4.2.1. Satellites

A comparison of LIMA/ice results with satellite observations of PMC and an interhemispheric comparison is somewhat problematic since various instrumental effects need to be taken into account, for example wavelengths, observation geometry, geographical coverage, sampling restrictions given by satellite orbit, tidal effects, long term changes, etc. In particular different scattering angles (forward versus backward) lead to a large difference in detected radiances and therefore presumably also in occurrence frequencies. It is clear from the results presented above that a bias in seasonal and/or geographical coverage may have a severe effect on a NH/SH comparison of PMC. Despite these limitations we will compare some satellite results with our LIMA/ice calculation of BSC, i.e., the backscatter properties of ice layers for $\lambda = 532\,\mathrm{nm}$ which, strictly speaking, is applicable for a lidar only. We argue that the main features are presumably also relevant for satellite instruments relying on scattering at similar or shorter wavelengths. A more detailed comparison taking into account the specific setup for a given satellite instrument will be performed in the future.

There is a long history of PMC observations with several instruments on different satellites. DeLand et al. (2006) have recently published an excellent overview of available instruments and measurements. The longest record stems from the SBUV instruments on various NOAA satellites and from the UV spectrometer on the SME satellite. Olivero and Thomas (1986) performed a comprehensive study of PMC from SME and found that the occurrence frequencies in the NH and SH are quite similar in the 1981–1984 period. An analytic representation of the latitudinal and seasonal occurrence rate of SME data is now available and confirms the similarity, but also shows some small differences, for example a longer NH season (E. Shettle, private communication). On the other hand, SBUV measurements persistently show more PMC in the NH for more than 20 years with very few exceptions (Thomas, 1991). Smaller PMC extinctions in the SH were found in HALOE data (Hervig and Siskind, 2006; Wrotny and Russell, 2006). Comparison with simultaneously measured temperatures suggests a warmer SH. It should be noted, however, that temperatures from HALOE at PMC altitudes are somewhat uncertain due to radiation contamination by ice particles.

Bailey et al. (2005) found that PMC occurrence frequencies observed by the Student Nitric Oxide Explorer (SNOE) are larger in the NH compared to the SH, whereas the difference increases toward lower latitudes. SNOE clearly shows a hemispheric difference in the latitudinal extent of PMC occurrence rates: PMC reach to 55°N and only to 60−65°S, a result already observed by SME (Thomas and Olivero, 1989). These observations nicely confirm our LIMA/ice results. PMC are also dimmer in the SH, again consistent with LIMA/ice. As noted in Bailey et al. (2005) the NH/SH differences observed by SNOE are significantly larger compared to SME which may be caused by instrumental and/or by geophysical effects (e.g. seasonal and geographical coverage, long term changes, etc.). The NH/SH comparison of PMC with SNOE suffers from the difference in scattering angles, similar to SME. However, in a specific experiment the SNOE satellite was turned such that it observed PMC under the same scattering angle in both hemispheres (Bailey et al., 2007). These measurements basically confirm the main results stated above. It is interesting to note that the seasonal variation of PMC altitude from SNOE resembles the main characteristics shown in Fig. 12, namely higher altitudes at the beginning and end of the season (see Figure 6 in Bailey et al., 2005). The authors hesitate to compare PMC altitudes in the SH/NH from SNOE because of different scattering geometry. A comprehensive study of SH/NH PMC altitudes from HALOE has recently been published by Wrotny and Russell (2006). Combining data from all 14 years and latitudes between 55° and 70° they find the mean PMC ~0.9 km lower in the NH, consistent with LIMA/ice.

Interhemispheric differences in PMC brightness and mean altitude are also reported from the ODIN satellite (Petelina et al., 2006). Again, NH PMC are brighter and more frequent compared to the SH. Furthermore, they appear 1 km higher in the SH. Some evidence is found that part of the NH/SH PMC difference is due to interhemispheric stratosphere–mesosphere coupling (Karlsson et al., 2007).

We summarize that there is substantial evidence that PMC in the SH are systematically less frequent, less bright, extent less equator-ward, and are found at somewhat higher altitudes compared to the NH. We note that all these features are seen in LIMA/ice, some with a remarkable degree of compliance.

4.2.2. Radars (PMSE)

We have seen from Figs. 4 and 7 that the general seasonal and latitudinal variation of PMSE from LIMA/ice agrees with observations. In particular at the Antarctic station Machu Picchu (62°S) PMSE are expected to be very seldom. They should occur much more frequently at similar NH stations. Indeed, first detections of PMSE came from midlatitudes in the NH (namely at Lindau, 52°N and Poker Flat 65°N), whereas similar instruments failed or detected much weaker PMSE at SH latitudes (Czechowsky et al., 1979; Ecklund and Balsley, 1981; Balsley et al., 1993; Woodman et al., 1999). A VHF radar was recently installed at the SH polar latitude station Davis (68°S, 78°E) and indeed detects PMSE quite often, similar to the NH (Morris et al., 2004; Bremer et al., 2006). This is in nice agreement with LIMA/ice stating that the NH/SH difference in PMSE occurrence rates decreases towards higher latitudes.

LIMA/ice predicts that the PMSE season terminates earlier in the SH than in the NH (see Fig. 4). Latteck et al. (2007) have recently compared NH/SH PMSE from ALOMAR/Davis after careful calibration of both VHF radars. Indeed they find that the SH season ends earlier compared to NH by approximately 20 days. It should be noted that in this terminology the 'end of season' in the SH is marked by a large drop of PMSE signal strength, but still some weak PMSE are present after that time. A comparison with the seasonal variation of temperature differences measured by FS indicates that the difference in PMSE is primarily caused by an early transition of the thermal structure in the SH from summer to autumn conditions (see Fig. 6 in Lübken et al., 2004a). In mid-February at 68°S the mesopause is already more than 10° warmer compared to mid-August at 69°N, whereas the difference is very small in January/July. We note that both LIMA/ice and the observations show a similar start of the PMSE season in both hemispheres and an earlier end in the SH. The dates when the season starts are somewhat late in LIMA/ice (in both hemispheres) compared to observations. We repeat that several geophysical factors influence PMSE which are not covered by the PMSE proxy introduced above, for example turbulence, enhanced ionization by geomagnetic and/or solar activity, etc. We will investigate the cause of this slight discrepancy in more detail in the future.

We conclude that LIMA/ice reproduces the main PMSE features as observed by several VHF radars in the NH and SH, respectively. The NH/SH similarities and differences of PMSE are most likely determined by the thermal structure, whereas other potential reasons, such as turbulence, meteoric smoke particles, ionization, etc., play a minor role.

4.2.3. Lidar (NLC)

Some lidar measurements of NLC have been performed in the SH but the data base is still patchy compared to the NH where more than thousand hours of NLC observations are available (Chu et al., 2004, 2006; Hansen et al., 1989; Thayer et al., 1995; Fiedler et al., 2003; Höffner et al., 2003; Gerding et al., 2007). A careful intercomparison requires consideration of various observational parameters, such as lidar sensitivity, wavelength, daylight capability, seasonal coverage, interference from metal atoms, etc. This is beyond the scope of this paper. We will ignore any potential systematic instrumental effect on the NH/SH difference of NLC in the following. In a recent overview Chu et al. (2006) report an overall mean NLC centroid altitude of 84.1 km at Rothera (68°S) for 3 seasons, with a year-to-year variation of mean altitudes of up to 1 km. At these latitudes LIMA/ice indeed finds the NLC approximately 1 km higher in the SH (see Fig. 3). We note that a complete seasonal coverage of SH NLC within a single year is not yet available. We have stated earlier that NLC characteristics, for

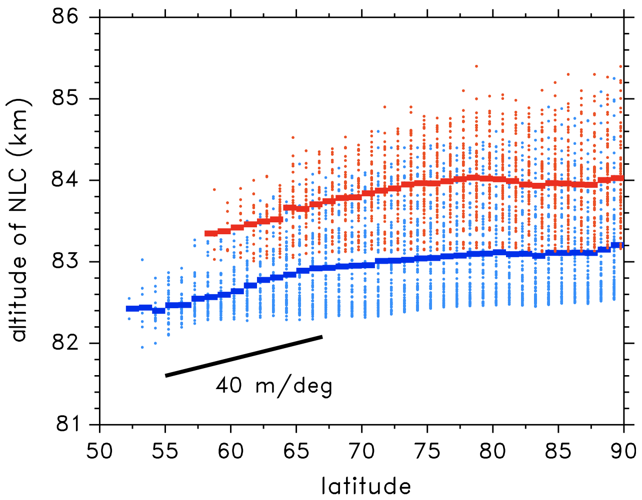

Fig. 14. Daily zonal mean NLC centroid altitudes (dots) with BSC$>4\times10^{-10}$/(sr m) as a function of latitude during the NLC seasons in 2001 (NH, blue) and 2004/05 (SH, red). The seasonal variation of these data is shown in Fig. 12. The thick lines present the means over the entire season. A slope of 40 m/deg is indicated to reflect lidar measurements presented in Chu et al. (2006).

example the mean altitude, varies with season, and also from year to year. Chu et al. (2006) also compare mean NLC altitudes from various lidars in the NH and SH, respectively (see their Figure 3). In Fig. 14 we show a similar analysis using LIMA results. This figure demonstrates the large variability but also some systematic similarities with observations. For example, mean altitudes are generally larger in the SH by $\sim$0.6$-$1.0 km. Altitudes increase with latitude with a slope close to 40 m/deg (smaller at very high latitudes). These results are in nice agreement with observations except for the mean NLC height at the South Pole which is systematically smaller in LIMA ($\sim$84 km) compared to observations (84.9 km). We note that the observed mean NLC altitudes at the South Pole varied by nearly 1 km between the two seasons when measurements are available. We will further investigate NLC characteristics in LIMA and compare with lidar observations in the future.

5. Conclusion and outlook

We have presented results from LIMA/ice which is a combination of a 3-d GCM model with a simulation of ice particle generation, growth, transport, sublimation, etc. Water vapor in the model is interactively coupled to ice particles thereby causing significant redistribution of H_2O (‘freeze drying’). In the troposphere and lower stratosphere LIMA is coupled to the wind and temperature fields from ERA-40. For the NH/SH comparison we have used the ERA-40 fields from the corresponding hemisphere, but we have applied the same trace gas distribution and chemistry in both hemispheres. The SH summer mesosphere is slightly warmer in LIMA (by a few degrees) and the difference increases with decreasing latitude. We find that the eccentricity of Earth’s orbit generates a significant part of this difference. NH/SH temperature differences in LIMA are consistent with in situ measurements from falling spheres performed in both hemispheres. Compared to other models our temperature differences are small but still generate the observed NH/SH differences in ice layer characteristics. We conclude that even small temperature deviations in both hemispheres can lead to substantially different ice layer characteristics. It should be noted, though, that ice particles start to nucleate around the mesopause (where temperature differences are larger) and may have been transported several hundred kilometers encountering different atmospheric conditions before they finally are observed as NLC. Therefore, the local temperature difference at NLC altitudes may not be essential for a NH/SH difference in NLC characteristics.

Ice layers are more frequent and brighter in the NH (at all latitudes) and extend further equatorward in the NH compared to SH. The season ends earlier in the SH compared to NH. Ice particle altitudes vary with season and are higher in the SH by approximately 0.6–1 km.

We conclude that temperature is the main driver for the observed NH/SH differences. The NH/SH temperature difference varies from year to year. This means that a NH/SH comparison of ice layer observations from a single year may not reflect the mean difference in the thermal structure. Furthermore, temperatures and ice layers vary differently with latitude and season in the SH and NH hemisphere. This implies that intercomparisons of measurements and/or models are not meaningful if they are taken from significantly different or from too extended latitude ranges.

We note that the main features of interhemispheric PMSE differences are reproduced by LIMA/ice. This implies that other factors required for PMSE (turbulence, ionization, nucleation particles, water vapor, etc.) play a minor role for PMSE or are rather similar in both hemispheres. This is somewhat surprising considering a potential difference in gravity wave generation and filtering and meteoric influx.

It should be kept in mind that we have mainly used ice layer results from two years when the NH/SH temperature differences is somewhat larger compared to the mean. In the future we intend to run the sophisticated LIMA/ice version (with 20 million dust/ice particles) for several years and study inter-annual variability and solar cycle effects. It remains to be seen which interhemispheric similarities and differences are persistent. We will also introduce some improvements, for example a seasonally varying water vapor concentration at the latitudinal and height boundary of the ice domain. We intend to make a more realistic comparison with several satellite measurements taking into account the specific observation conditions, such as scattering angle, wavelength etc. Furthermore, we will study in detail the physical mechanism causing the NH/SH temperature difference, e.g. by characterizing the influence of dynamics on the upper mesosphere and the NH/SH temperature difference.

Acknowledgments

We thank Gerd Baumgarten and Florian Herbort for their assistance in running and analyzing the LIMA/ice data, Jens Fiedler for an update of the NLC observations from ALOMAR, and Ralph Latteck for the PMSE data in Fig. 4. This project is supported by the Deutsche Forschungsgemeinschaft under the CAWSES SPP Grant LU 1174/3-1 (SOLEIL).

References

Bailey, S.M., Merkel, A.W., Thomas, G.E., Carstens, J.N., 2005. Observations of polar mesospheric clouds by the Student Nitric Oxide Explorer. Journal of Geophysical Research 110 (D13), doi:10.1029/2004JD005422, eid: D13203.

Bailey, S.M., Merkel, A.W., Thomas, G.E., Rusch, D., 2007. Hemispheric differences in Polar Mesospheric Cloud morphology observed by the Student Nitric Oxide Explorer. Journal of Atmospheric and Solar Terrestrial Physics 69, 1407–1418, doi:10.1016/j.jastp.2007.02.008.

Balsley, B.B., Woodman, R.F., Sarango, M., Urbina, J., Rodriguez, R., Ragaini, E., Carey, J., 1993. Southernhemisphere PMSE: where are they? Geophysical Research Letters 20, 1983–1985, doi:10.1029/93GL02244.

Becker, E., Schmitz, G., 2003. Climatological effects of orography and land–sea heating contrasts on the gravity wave-driven circulation of the mesosphere. Journal of Atmospheric Science 60, 103–118.

Becker, E., Müllemann, A., Lübken, F.-J., Körnich, H., Hoffmann, P., Rapp, M., 2004. High Rossby-wave activity in austral winter 2002: modulation of the general circulation of the MLT during the MaCWAVE/MIDAS northern summer program. Geophysical Research Letters 31 (24), doi:10.1029/2004GL019615, eid: L24S03.

Berger, U., 2007. Modeling of middle atmosphere dynamics with LIMA. Journal of Atmospheric and Solar Terrestrial Physics, submitted for publication.

Berger, U., Lübken, F.-J., 2006. Weather in mesospheric ice layers. Geophysical Research Letters 33 (4), doi:10.1029/2005GL024841, eid: L04806.

Berger, U., von Zahn, U., 2002. Icy particles in the summer mesopause region: three-dimensional modeling of their environment and two-dimensional modeling of their transport. Journal of Geophysical Research 107 (A11), doi:10.1029/2001JA000316, eid: 1366.

Berger, U., von Zahn, U., 2007. Three-dimensional modeling of the trajectories of visible noctilucent cloud particles: An indication of particle nucleation well below the mesopause. Journal of Geophysical Research, 112 (D16), doi:10.1029/2006JD008106, eid: D16204.

Bremer, J., Hoffmann, P., Höffner, J., Latteck, R., Singer, W., Zecha, M., Zeller, O., 2006. Long-term changes of mesospheric summer echoes at polar and middle latitudes. Journal of Atmospheric and Solar Terrestrial Physics 68, 1940–1951, doi:10.1016/j.jastp.2006.02.012.

Carbary, J.F., Morrison, D., Romick, G.J., 2001. Hemispheric comparison of PMC altitudes. Geophysical Research Letters 28, 725–728.

Chu, X., Nott, G.J., Espy, P.J., Gardner, C.S., Diettrich, J.C., Clilverd, M.A., Jarvis, M.J., 2004. Lidar observations of polar mesospheric clouds at Rothera, Antarctica, 67.5°S, 68.0°W. Geophysical Research Letters 31 (02), doi:10.1029/2003GL018638, eid: L02114.

Chu, X., Espy, P.J., Nott, G.J., Diettrich, J.C., Gardner, C.S., 2006. Polar mesospheric clouds observed by an iron Boltzmann lidar at Rothera (67.5°S, 68.0°W), Antarctica from 2002-2005: properties and implications. Journal of Geophysical Research D20213 (D20), doi:10.1029/2006JD007086.

Czechowsky, P., Rüster, R., Schmidt, G., 1979. Variations of mesospheric structures in different seasons. Geophysical Research Letters 6, 459–462.

DeLand, M., Shettle, E.P., Thomas, G.E., Olivero, J.J., 2006. A quarter-century of satellite polar mesospheric cloud observations. Journal of Atmospheric and Solar Terrestrial Physics 68, 9–29, doi:10.1016/j.jastp.2005.08.003.

Donahue, T.M., Guenther, B., Blamont, J.E., 1972. Noctilucent clouds in daytime: circumpolar particulate layers near the summer mesopause. Journal of Atmospheric Science 29, 1205–1209.

Ecklund, W., Balsley, B., 1981. Long-term observations of the Arctic mesosphere with the MST radar at Poker Flat, Alaska. Journal of Geophysical Research 86, 7775–7780.

Fiedler, J., Baumgarten, G., von Cossart, G., 2003. Noctilucent clouds above ALOMAR between 1997 and 2001: occurrence and properties. Journal of Geophysical Research 108 (D8), doi:10.1029/2002JD002419, eid: 8453.

Fiedler, J., Baumgarten, G., von Cossart, G., 2005. Mean diurnal variations of noctilucent clouds during 7 years of lidar observations at ALOMAR. Annales Geophysicae 23, 1175–1181.

Gerding, M., Höffner, J., Rauthe, M., Singer, W., Zecha, M., Lübken, F.-J., 2007. Simultaneous observation of NLC, MSE and temperature at a mid-latitude station 54°N. Journal of

Geophysical Research 112 (D12), doi:10.1029/2006JD008135, eid: D12111.

Goldberg, R.A., Fritts, D.C., Williams, B.P., Lübken, F.-J., Rapp, M., Singer, W., Latteck, R., Hoffmann, P., Mann, A., Baumgarten, G., Schmidlin, F.J., She, C.-Y., Krueger, D.A., 2004. The MacWAVE/MIDAS rocket and ground-based measurement of polar summer dynamics: overview and mean state structure. Geophysical Research Letters 31 (24), doi:10.1029/2004GL019411, eid: L24S02.

Hansen, G., Serwazi, M., von Zahn, U., 1989. First detection of a noctilucent cloud by lidar. Geophysical Research Letters 16, 1445–1448.

Hervig, M., Siskind, D., 2006. Decadal and inter-hemispheric variability in polar mesospheric clouds, water vapor, and temperature. Journal of Atmospheric and Solar Terrestrial Physics 68, 30–41, doi:10.1016/j.jastp.2005.08.010.

Höffner, J., Fricke-Begemann, C., Lübken, F.-J., 2003. First observations of noctilucent clouds by lidar at Svalbard, 78°N. Atmospheric Chemistry and Physics 3, 1101–1111.

Hunten, D.M., Turco, R.P., Toon, O.B., 1980. Smoke and dust particle of meteoric origin in the mesosphere and stratosphere. Journal of Atmospheric Science 37, 1342–1357.

Karlsson, B., Körnich, H., Gumbel, J., 2007. Evidence for interhemispheric stratosphere–mesosphere coupling derived from noctilucent cloud properties. Geophysical Research Letters 34 (16), doi:10.1029/2007GL030282, eid: L16806.

Kutepov, A.A., Feofilov, A.G., Marshall, B.T., Gordley, L.L., Pesnell, W.D., Goldberg, R.A., III, J.M.R., 2006. SABER temperature observations in the summer polar mesosphere and lower thermosphere: importance of accounting for the CO_2 v_2 quanta VV exchange. Geophysical Research Letters 33 (21), doi:10.1029/2006GL026591, eid: L21809.

Latteck, R., Singer, W., Morris, R.J., Holdsworth, D.A., Murphy, D.J., 2007. Observation of polar mesosphere summer echoes with calibrated VHF radars at (69° N) in the northern and southern hemispheres. Geophysical Research Letters 34 (14), doi:10.1029/2007GL030032, eid: L14805.

Leslie, R.C., 1885. Sky glows. Nature 32, 245.

Lübken, F.-J., 1997. Seasonal variation of turbulent energy dissipation rates at high latitudes as determined by in situ measurements of neutral density fluctuations. Journal of Geophysical Research 104, 13,441–13,456.

Lübken, F.-J., 1999. Thermal structure of the Arctic summer mesosphere. Journal of Geophysical Research 104 (D8), 9135–9149.

Lübken, F.-J., Fricke, K.-H., Langer, M., 1996. Noctilucent clouds and the thermal structure near the Arctic mesopause. Journal of Geophysical Research 101 (D5), 9489–9508.

Lübken, F.-J., Müllemann, A., Jarvis, M.J., 2004a. Temperatures and horizontal winds in the Antarctic summer mesosphere. Journal of Geophysical Research 109 (D24), doi:10.1029/2004JD005133, eid: D24112.

Lübken, F.-J., Zecha, M., Höffner, J., Röttger, J., 2004b. Temperatures, polar mesosphere summer echoes, and noctilucent clouds over Spitsbergen (78°N). Journal of Geophysical Research 109 (D11), doi:10.1029/2003JD004247, eid: D11203.

Lübken, F.-J., Rapp, M., Strelnikova, I., 2007. The sensitivity of mesospheric ice layers to atmospheric background temperatures and water vapor. Advances in Space Research 40, doi:10.1016/j.asr.2007.01.014, 794–801.

Mauersberger, K., Krankowsky, D., 2003. Vapor pressure above ice at temperatures below 170 K. Geophysical Research Letters 30 (3), doi:10.1029/2002GL016183, eid: 1121.

Morris, R.J., Murphy, D.J., Reid, I.M., Holdsworth, D.A., Vincent, R.A., 2004. First polar mesosphere summer echoes observed at Davis, Antarctica (68.6°S). Geophysical Research Letters 31 (16), doi:10.1029/2004GL020352, eid: L16111.

Müllemann, A., Lübken, F.-J., 2005. Horizontal winds in the mesosphere at high latitudes. Advances in Space Research 35 (11), 1890–1894, doi:10.1016/j.asr.2004.11.014.

Murphy, D.M., Koop, T., 2005. Review of the vapour pressure of ice and supercooled water for atmospheric applications. Quarterly Journal of the Royal Metereological Society 131, 1539–1565.

Olivero, J.J., Thomas, G.E., 1986. Climatology of polar mesospheric clouds. Journal of Atmospheric Science 43, 1263–1274.

Petelina, S.V., Llewellyn, E.J., Degenstein, D.A., Lloyd, N.D., 2006. Odin/OSIRIS limb observations of polar mesospheric clouds in 2001–2003. Journal of Atmospheric and Solar Terrestrial Physics 68, 42–55, doi:10.1016/j.jastp.2005.08.004.

Rapp, M., Lübken, F.-J., 2004. Polar mesosphere summer echoes (PMSE): review of observations and current understanding. Atmospheric Chemistry and Physics 4, 2601–2633.

Rapp, M., Thomas, G.E., 2006. Modeling the microphysics of mesospheric ice particles: Assessment of current capabilities and basic sensitivities. Journal of Atmospheric and Solar Terrestrial Physics 68, 715–744, doi:10.1016/j.jastp.2005.10.015.

Rapp, M., Lübken, F.-J., Hoffmann, P., Latteck, R., Baumgarten, G., Blix, T., 2003. PMSE dependence on aerosol charge number density and aerosol size. Journal of Geophysical Research 108 (D8), 8441, doi:10.1029/2002JD002650, eid: 8441.

Seele, C., Hartogh, P., 1999. Water vapor of the polar middle atmosphere: annual variation and summer mesosphere conditions as observed by ground-based microwave spectroscopy. Geophysical Research Letters 26, 1517–1520.

Siskind, D.E., Eckerman, S., McCormack, J.P., Backmeister, M.A.J., 2003. Hemispheric differences in the temperature of the summertime stratosphere and mesosphere. Journal of Geophysical Research 108 (D2), doi:10.1029/2002JD002095, eid: 4051.

Siskind, D.E., Stevens, M.H., Englert, C.R., 2005. A model study of global variability in mesospheric cloudiness. Journal of Atmospheric and Solar Terrestrial Physics 67, 501–513, doi:10.1016/j.jastp.2004.11.007.

Sonnemann, G.R., Grygalashvyly, M., 2005. Solar influence on mesospheric water vapor with impact on NLCs. Journal of Atmospheric and Solar Terrestrial Physics 67, 177–190, doi:10.1016/j.jastp.2004.07.026.

Stevens, M.H., Meier, R.R., Chu, X., DeLand, M.T., Plane, J.M.C., 2005. Antarctic mesospheric clouds formed from space shuttle exhaust. Geophysical Research Letters 32 (13), doi:10.1029/2005GL023054, eid: L13810.

Thayer, J.P., Nielsen, N., Jacobsen, J., 1995. Noctilucent cloud observations over Greenland by a Rayleigh lidar. Geophysical Research Letters 22, 2961–2964, doi:10.1029/95GL02126.

Thomas, G.E., 1984. Solar Mesosphere Explorer measurements of polar mesospheric clouds noctilucent clouds. Journal of Atmospheric Terrestrial Physics 46, 819–824.

Thomas, G.E., 1991. Mesopheric clouds and the physics of the mesopause region. Reviews of Geophysics 29 (4), 553–575, doi:10.1029/91RG01604.

Thomas, G.E., Olivero, J.J., 1989. Climatology of polar mesospheric clouds. 2. further analysis of Solar Mesosphere Explorer data. Journal of Geophysical Research 94 (D12), 14,673–14,681, doi:10.1029/88JD04040.

von Savigny, C., Sinnhuber, M., Bovensmann, H., Burrows, J. P., Kallenrode, M.-B., Schwartz, M., 2007. On the disappearance of noctilucent clouds during the January 2005 solar proton events. Geophysical Research Letters 34 (02), doi:10.1029/2006GL028106, eid: L02805.

von Zahn, U., Berger, U., 2003. Persistent ice cloud in the midsummer upper mesosphere at high latitudes: three-dimensional modeling and cloud interactions with ambient water vapor. Journal of Geophysical Research 108 (D7), doi:10.1029/2002JD002409, edi: 8451.

Woodman, R.F., Balsley, B.B., Aquino, F., Flores, L., Vazquez, E., Sarango, M., Huamann, M.M., Soldi, H., 1999. First observations of polar mesosphere summer echoes in Antarctica. Journal of Geophysical Research 104 (A10), 22577–22590, doi:10.1029/1999JA900226.

Wrotny, J.E., Russell, J.M., 2006. Interhemispheric differences in polar mesospheric clouds observed by the HALOE instrument. Journal of Atmospheric and Solar Terrestrial Physics 68 (12), 1352–1369, doi:10.1016/j.jastp.2006.05.014.

Zecha, M., Bremer, J., Latteck, R., Singer, W., Hoffmann, P., 2003. Properties of midlatitude mesosphere summer echoes after three seasons of VHF radar observations at 54°N. Journal of Geophysical Research 108 (D8), doi:10.1029/2002JD002442, eid: 8439.